ARTICLE NO. 79-1454R

J 80 - 176

Navier-Stokes Solutions for Spin-Up in a Filled Cylinder

20005
20006
20019

Clarence W. Kitchens Jr.*
U.S. Army Armament Research and Development Command, Aberdeen Proving Ground, Md.

A predictor-corrector multiple-iteration scheme is adapted and used to solve the unsteady Navier-Stokes equations. Numerical solutions for Reynolds numbers up to 50,000 are obtained for the transient spin-up flow in a cylindrical container. The grid point distribution is optimized using coordinate transformations to resolve simultaneously details of both the interior and endwall/sidewall boundary-layer flows formed during spin-up. Calculations for five test problems show very good agreement with previous computations and experimental measurements. Transient phenomena occurring at early time near the sidewall, including reversed flow regions and inertial oscillations, are discussed as well as certain aspects of the endwall Ekman layer flow.

Nomenclature

a	= cylinder radius
$b,\bar{c},d,e$	= coordinate transformation constants
c	= cylinder half-height
Ek	= Ekman number $[=\nu/(\Omega c^2)]$
r,R	= nondimensional and dimensional radial coordinate
Re	= Reynolds number $[=\Omega a^2/\nu]$
t,T	= nondimensional and dimensional time $(t=\Omega T)$
u,v,w	= r,θ,z nondimensional velocity components
z,Z	= nondimensional and dimensional axial coordinate
α	= cylinder aspect ratio $[=c/a]$
β	= transformed radial coordinate
γ,Γ	= nondimensional and dimensional circulation
ϵ_i	= iteration convergence criteria
ζ,Z	= nondimensional and dimensional vorticity
η	= transformed axial coordinate
θ	= azimuthal coordinate
ν	= liquid kinematic viscosity
ψ,Ψ	= nondimensional and dimensional stream function
Ω	= final cylinder rotation rate
Ω_i	= initial cylinder rotation rate
$\Delta\beta,\Delta\eta$	= grid sizes in β and η coordinates
Δt	= time step

Superscripts

m	= γ,ζ—iteration level
n	= ψ—iteration level

Introduction

THE objective of this work is to develop an accurate numerical procedure for solving the unsteady Navier-Stokes equations to describe transient spin-up flow occurring in a cylindrical container when it is suddenly rotated about its longitudinal axis. Knowledge of this internal flow is needed to design gun-launched projectiles which carry smoke/incendiary agents or chemical payloads. Liquid payloads enhance spin decay of projectiles[1,2] and their presence can produce flight dynamic instabilities as a result of resonance between the projectile nutational motion and inertial oscillations in the rotating liquid.[3] From a computational viewpoint this problem is instructive because it is an example of a class of internal flow problems for which computational experiments can uncover details of the flow that cannot be easily visualized or measured experimentally.

The results presented here demonstrate that a predictor-corrector multiple-iteration (PCMI) technique developed by Rubin and Lin[4] for solving steady three-dimensional boundary region problems can be successfully adapted to solve the unsteady Navier-Stokes equations. In the present approach this method is combined with the Gauss-Seidel procedure[5] and grid-stretching transformations to produce an accurate procedure for describing the spin-up process. Calculations with the PCMI method have been performed for spin-up from rest and spin-up from an initial state of solid-body rotation. Numerical results have been obtained for a range of cylinder aspect ratios α of 0.3-4.4 and a range of Reynolds numbers of 215-50,000. Calculations performed for five test problems show very good agreement with previous computations[6-8] and experimental measurements.[6,9] Numerical results have been used[10] to quantify the flow in the Ekman (or endwall) boundary layers during spin-up from rest and develop an appropriate compatibility condition for use in Wedemeyer's spin-up model.[1] Neitzel[11] successfully used the PCMI procedure developed in the present work to study the onset and temporal development of fluid dynamic instabilities during spin down in a cylinder.

Governing Equations and Boundary Conditions

The calculations employ a finite-difference analog of the unsteady axisymmetric Navier-Stokes equations formulated in cylindrical coordinates (r,θ,z). The equations are expressed in terms of ψ,ζ, and γ instead of velocity and pressure in order to simplify the numerical procedure. In dimensionless variables the governing equations are

$$\nabla^2\psi-\psi_r/r=r\zeta \tag{1}$$

$$\zeta_t+u\zeta_r+w\zeta_z-u\zeta/r-2\gamma\gamma_z/r^3=(1/Re)[\nabla^2\zeta+\zeta_r/r-\zeta/r^2] \tag{2}$$

$$\gamma_t+u\gamma_r+w\gamma_z=(1/Re)[\nabla^2\gamma-\gamma_r/r] \tag{3}$$

where the subscripts denote partial differentiation and

$$Re=\Omega a^2/\nu \tag{4}$$

$$\nabla^2=\partial^2/\partial r^2+\partial^2/\partial z^2 \tag{5}$$

$$\gamma=rv \tag{6}$$

$$\zeta=u_z-w_r \tag{7}$$

Presented as Paper 79-1454 at the AIAA Computational Fluid Dynamics Conference, Williamsburg, Va., July 23-25, 1979; submitted Aug. 10, 1979; revision received Jan. 21, 1980. This paper is declared a work of the U.S. Government and therefore is in the public domain.

Index categories: Computational Methods; Viscous Nonboundary-Layer Flows; Hydrodynamics.

*Acting Chief, Target Loading and Response Branch, Terminal Ballistics Division, Ballistic Research Laboratory. Member AIAA.

with the axisymmetric stream function defined so that

$$u=\psi_z/r \text{ and } w=-\psi_r/r \tag{8}$$

The Ekman number based upon half-height is related to Re by

$$Ek=\nu/(\Omega c^2)=1/(\alpha^2 Re) \tag{9}$$

The stream function-vorticity-circulation formulation yields an elliptic partial differential equation (PDE) [Eq. (1)] and two parabolic PDEs [Eqs. (2) and (3)] which are coupled. The boundary conditions impose additional coupling between ψ and ζ.

The nondimensional variables used here are defined by

$$r=R/a,\ z=Z/a,\ t=\Omega T,\ u=U/(\Omega a),\ v=V/(\Omega a),\ w=W/(\Omega a),\ \psi=\Psi/(\Omega a^3),\ \gamma=\Gamma/(\Omega a^2),\ \zeta=Z/\Omega \tag{10}$$

The initial conditions for spin-up are

$$\psi=\zeta=0,\ \gamma=\Omega_i r^2/\Omega \text{ for } t\leq 0 \tag{11}$$

Computational efficiency and resolution are improved by employing a symmetry boundary condition at the cylinder midplane, $z=\alpha$. This effectively halves the number of grid points required. The boundary conditions for $t\geq 0$ are

$$\psi(t,0,z)=\gamma(t,0,z)=\zeta(t,0,z)=0 \tag{12}$$

$$\psi(t,1,z)=0,\ \gamma(t,1,z)=1,\ \zeta(t,1,z)=\psi_{rr}(t,1,z) \tag{13}$$

$$\psi(t,r,0)=0,\ \gamma(t,r,0)=r^2,\ \zeta(t,r,0)=\psi_{zz}(t,r,0)/r \tag{14}$$

$$\psi(t,r,\alpha)=\zeta(t,r,\alpha)=0,\ \gamma_z(t,r,\alpha)=0 \tag{15}$$

The boundary conditions for vorticity along the sidewall and endwall [Eqs. (13) and (14)] are derived from Eqs. (7) and (8) by imposing the no-slip conditions for velocity. Figure 1 illustrates the coordinate system and boundaries used in the numerical calculations.

During spin-up there are viscous regions near the sidewall and endwalls which become very thin as Re becomes larger than 1000 or so, necessitating a fine grid to resolve the boundary-layer type phenomena along these walls. Analytical coordinate transformations[12]

$$\beta=\frac{\ln[(b+r)/(b-r)]}{\ln[(b+1)/(b-1)]} \tag{16}$$

$$\eta=1+\frac{\ln[(\bar{c}+z/\alpha-1)/(\bar{c}-z/\alpha+1)]}{\ln[(\bar{c}+1)/(\bar{c}-1)]} \tag{17}$$

with $b=(1-d)^{-1/2}$ and $\bar{c}=(1-e)^{-1/2}$ are used to optimize the grid point placement and transform a nonuniform grid in the physical plane into an equally spaced grid in the computational plane. Figure 2 shows a typical grid point distribution in the physical plane produced with Eqs. (16) and (17). The complete set of transformed equations and boundary conditions is given in Ref. 10.

Discussion of Numerical Procedure

Several methods have been used by previous investigators to solve the stream function-vorticity form of the Navier-Stokes equations. Perhaps the most popular technique is to combine the alternating direction implicit (ADI) method[13] for the ζ and γ equations with either an ADI or successive over-relaxation (SOR) method[14] for the ψ equation. Briley[7,8] applied the former approach to spin-up in a cylinder. In the present approach a semi-implicit PCMI method is used to solve the ζ and γ equations and the Gauss-Seidel method[5] is used to solve the ψ equation.

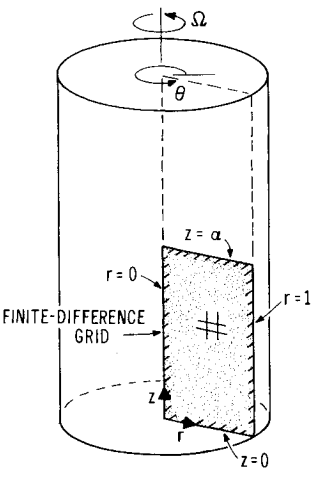

Fig. 1 Geometry for spin-up calculations.

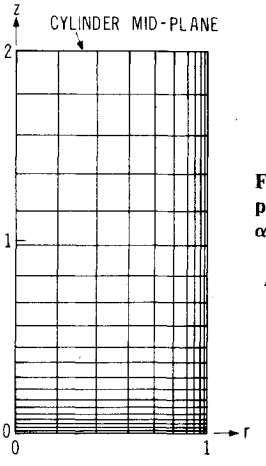

Fig. 2 Typical grid point distribution in physical plane for coarse 11×21 grid with $\alpha=2$ and $d=e=0.05$.

The PCMI technique was adopted for this unsteady problem because the present author's prior experience[15] showed the method to be reliable and easy to implement. Rubin and Lin[4] originally used the PCMI technique to investigate steady hypersonic viscous flow along a right-angle corner, imposing a symmetry condition along the diagonal. This resulted in the computation of large gradients in only one coordinate direction, which they treated implicitly. In the present application there are large gradients in two coordinate directions and some of the advantages of the PCMI technique are compromised. In adapting this technique to the present problem we chose to treat the radial direction implicitly to maintain consistency with previous work[2] based upon the Wedemeyer spin-up model. This choice was advantageous in studying the early-time flow development along the sidewall and in applying the symmetry boundary conditions at $z=\alpha$. It leads, however, to an explicit time step restriction, to be discussed below, that is governed by the large axial gradients in the endwall boundary layer.

In the present method all flow gradients in the z direction are approximated by prediction and subsequent correction in this time-iterative technique. This approach eliminates cross coupling of grid points, thus reducing the size of the inversion matrices and decreasing computer time. The iteration procedure allows the boundary vorticity to converge and also allows the nonlinear terms to be approximated and then corrected, giving a more accurate simulation of the nonlinear coupling between equations.

Central difference formulas are used for all spatial derivatives at interior points, avoiding false diffusion effects introduced by upwind difference schemes. Temporal derivatives are approximated by second-order accurate one-sided difference formulas involving three time levels. The

truncation errors for interior points are of $0(\Delta t^2, \Delta\beta^2, \Delta\eta^2)$. Reference 10 gives the complete set of finite-difference equations used in this work, together with a discussion of the manner in which the boundary conditions were implemented. It should be noted that a first-order form for the wall vorticity boundary conditions[10] was used to obtain the results discussed in this paper. Based on test calculations for $\alpha = 1$ and $Re = 1000$, the numerical technique appears to be fully compatible with second-order accurate wall vorticity expressions.

The numerical procedure is applied by using the PCMI method to solve the difference equations for γ^{m+1} and ζ^{m+1} using the m iterate values to form the coefficients of the nonlinear terms, where m denotes the γ and ζ iteration level. The calculations start along the row of points adjacent to the midplane and work downward toward the endwall (see Fig. 2). The derivatives in the β direction are treated implicitly, requiring the solution of a tridiagonal system of equations along each successive row.

At the end of each m iterative cycle the ψ difference equation is solved iteratively using the Gauss-Seidel method; the SOR method was used for test calculations but it did not speed up the overall procedure. The solution for ψ is obtained by starting at the interior grid point adjacent to $\beta = \eta = 0$ and sweeping first in β and then in η, making use of updated values as soon as they become available. Convergence of ψ is assumed when

$$|\psi^{n+1} - \psi^n| \leq \epsilon_1 \tag{18}$$

at every grid point, where n is the ψ iteration level. Convergence is typically achieved in 2-3 n iterations with $\epsilon_1 = 1 \times 10^{-7}$. The converged values for ψ are used to update the boundary values for ζ and repeat the iteration process for γ and ζ. The iteration process is assumed to converge when both

$$|\gamma^{m+1} - \gamma^m| \leq \epsilon_2 \tag{19}$$

$$|\zeta^{m+1} - \zeta^m| \leq \epsilon_3 \tag{20}$$

at every grid point. It typically requires 2-3 m iterations to satisfy Eqs. (19) and (20) with $\epsilon_2 = \epsilon_3 = 1 \times 10^{-4}$; at very early time 5-10 iterations are needed due to the severe flow unsteadiness caused by the impulsive start and the subsequent inaccuracy of the extrapolated guesses.

Stability Properties of Numerical Procedure

Rubin and Lin[4] have analyzed the interior point stability of the PCMI method for a linear model equation that approximates the unsteady two-dimensional Navier-Stokes equations. Their analysis shows that if iteration is not used the present PCMI technique has a stability restriction of the form $\Delta t < K\Delta\eta^2$, because the method is explicit in η; $\Delta\beta$ does not appear because β is treated implicitly. On the basis of their results for the case of repeated iteration, we conclude that the appropriate stability criterion for the present iterative scheme is

$$\Delta t \leq \min \left| \frac{\Delta\eta}{\eta_{zz}/Re + \beta_r \eta_z \psi_\beta / r} \right| \tag{21}$$

taken over all interior grid points. The term η_{zz}/Re results from the coordinate transformation in z; it vanishes if an equally spaced grid is used in the axial direction.

Since the results of such a linear stability analysis are inconclusive, we carried out test calculations to determine the validity of Eq. (21). These studies were conducted for $\alpha = 1$ and $Re = 1000$, 9742, and 50,000, using three combinations of grid sizes for each Re and several different transformation parameter combinations. The results show that numerical stability is always achieved when Eq. (21) is satisfied, even when equally spaced points are used. In limited cases numerical stability is achieved with Δt as large as 1.5 times the critical value predicted by Eq. (21). In general, the numerical studies confirm that the linear theory provides good guidance for the spin-up problem. Equation (21) was satisfied at each time step in the illustrative examples to be discussed next.

Comparison with Previous Work

The present method has been used to treat the problems of spin-up from rest and spin-up from an initial state of solid-body rotation. We compare our results with those of Warn-Varnas et al.,[6] for the latter problem. They used an ADI technique coupled with a scheme developed by Williams[16] to solve the velocity-pressure form of the Navier-Stokes equations. In their calculations they differenced the governing equations directly on a stretched grid instead of transforming to new coordinates. Their computations were verified by measurements taken with a laser doppler velocimeter (LDV) system.

Figure 3 shows a comparison of the present calculations with results from Ref. 6 (their Fig. 13b) in terms of their quantity called "zonal velocity" (ordinate in Fig. 3), which is a scaled nondimensional angular velocity. The results are shown at $r = 0.25$ on the cylinder symmetry plane for a case with $\alpha = 0.3182$, $Re = 7334$, and $\Omega_i = 0.8182\Omega$. The inertial oscillations excited by the sudden increase in cylinder rotation rate are clearly predicted in both computations and are in fairly good agreement with experimental measurements. Both of these numerical results appear to be within the experimental uncertainty associated with these data, according to the error analysis presented in Ref. 6. Comparisons for several other positions in the cylinder (not shown here) give similar agreement for both the decay of the zonal velocity and the amplitudes and phases of the inertial oscillations. The computation time and number of grid points used to obtain the numerical results in Ref. 6 are not stated. The PCMI

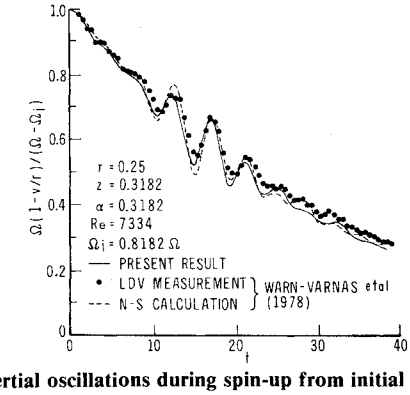

Fig. 3 Inertial oscillations during spin-up from initial state of rigid-body rotation.

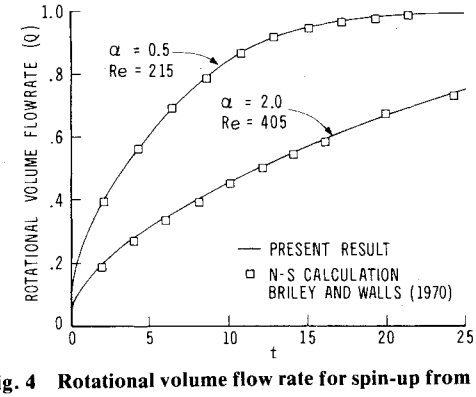

Fig. 4 Rotational volume flow rate for spin-up from rest.

calculations used a stretched ($d=0.3$, $e=0.1$) 41×21 ($r-z$) grid with 600 time steps ($\Delta t=0.063$). Approximately 2-3 m iterations, each consisting of 2-3 n iterations, were required per time step to satisfy Eqs. (18-20). The complete simulation represented in Fig. 3 required 52 s of CPU time on a CDC 7600 computer.

The problem of spin-up from rest has been emphasized in the present work because of its application to liquid-filled projectiles. This problem is nonlinear; the previous problem can be linearized for small $\Omega-\Omega_i$. Comparisons have been made with computations of Briley[7] and Briley and Walls[8] for spin-up from rest. They studied this problem for low Re using the ADI technique to solve the stream function-vorticity form of the Navier-Stokes equations. Figure 4 compares values of rotational volume flow rate,

$$Q=(1/\alpha)\int_0^1\int_0^{2\alpha} v\,dz\,dr \tag{22}$$

for two cases. The quantity Q can be used to obtain a measure of the spin-up time. Briley and Walls used a uniform grid that became restrictive at moderate Re due to the small thickness of the endwall boundary layers; they obtained results for Re as large as 1167. Our calculations appear to be in good agreement with all of their results for spin-up. Neitzel's comparisons for spin-down,[11] however, showed only qualitative agreement with Briley and Walls' results for $Re=1167$. The observed differences are thought to be due to grid size effects.

The present computations have also been compared with LDV measurements taken by Watkins and Hussey.[9] Figure 5 presents comparisons of azimuthal velocity along the cylinder midplane at four instants during spin-up for a case with $\alpha=1.515$, $Re=3076$. Figure 6 shows similar comparisons for $\alpha=1$, $Re=9741.6$. The size of the symbols used to plot the experimental data in Figs. 5 and 6 approximately represents the size of the error bars that should be attached to these data. The calculations in Fig. 6 used a 21×21 grid with $d=e=0.10$ and required 2745 time steps with $\Delta t=0.10$. Approximately 2 m iterations, each with 3 n iterations, were required to satisfy Eqs. (18-20), for a total CPU time of 69 s.

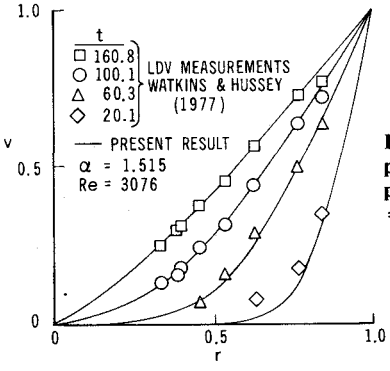

Fig. 5 Azimuthal velocity profiles at cylinder midplane for $\alpha=1.515$, $Re=3076$.

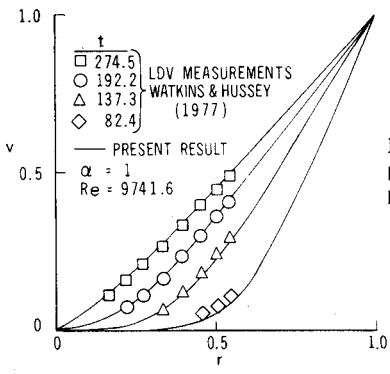

Fig. 6 Azimuthal velocity profiles at cylinder midplane for $\alpha=1$, $Re=9741.6$.

The results shown in Figs. 4-6 are representative of the "core" flow in Wedemeyer's model of spin-up from rest and they can be predicted fairly well using that model; the accuracy of the prediction increases as Re increases. However, Wedemeyer's model says very little about the flow in the corner region, along the sidewall, and in the Ekman layers. These phenomena will be discussed next.

Transient Phenomena during Spin-Up from Rest

The PCMI procedure has been used to study inertial oscillations and temporary regions of reversed secondary flow that develop and then subsequently decay during the initial stages of spin-up from rest. In a typical case[10] with $\alpha=0.3182$ and $Re=7334$, weak inertial oscillations develop in the flow adjacent to the sidewall immediately upon spin-up, decay in amplitude during the next few rotations, and become so weak that they cannot be detected at all for $t>40$. The phenomenon observed here is similar to thal indicated in Fig. 3, except that in this case the inertial oscillations are weaker and they occur only in the rotating fluid adjacent to the sidewall. The nonrotating fluid in the interior, for instance along the midplane at $r=0.25$ and $0\le t\le40$, cannot support such oscillations.

A second type of transient phenomenon that has been observed in these calculations is the formation of temporary reversed flow regions along the sidewall. These regions form during the first few rotations after the impulsive start and have been observed over the parameter range $1\le\alpha\le4.3$ and $1000<Re\le50{,}000$. Typical results for $\alpha=1$, $Re=9741.6$ are shown in Figs. 7-9 to illustrate the reversed flow formation and decay. Each figure shows instantaneous streamlines in one-fourth of the meridional plane, the cylinder midplane being the top boundary and the sidewall being the right boundary. The results were obtained with $d=e=0.1$ and $\Delta t=0.05$ using a 41×41 grid. The streamline contour interval is $\Delta\psi=0.0004$ for each figure with the wall value set to zero. The plots indicate that a counterclockwise meridional flow develops almost immediately after the impulsive start with no reversed flow regions present until approximately $t=6$. Figure 7 shows that a small reversed (clockwise) flow region has formed near the corner by $t=6$ as indicated by the small closed contour. By $t=13$ a second region forms, slightly higher up the sidewall from the one in Fig. 7. By $t=20$ (Fig. 8) there are four reversed flow regions present. During the next half rotation or so these reversed flow regions "collapse," or disappear, as indicated in Fig. 9 for $t=24$. They do not redevelop for $t>24$ and the rest of the spin-up process proceeds in a manner similar to that predicted by the Wedemeyer model.

The reversed flow regions do not develop in calculations for $\alpha=1$, $Re\le1000$, probably because of the larger amount of viscous dissipation. At higher Re there is less viscous dissipation present and inertial effects become more

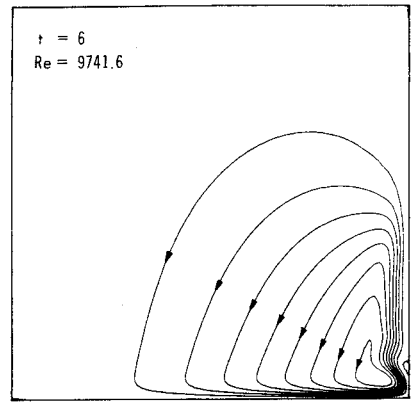

Fig. 7 Instantaneous streamlines at $t=6$; $\psi_{min}=-0.00003$, $\psi_{max}=0.00350$.

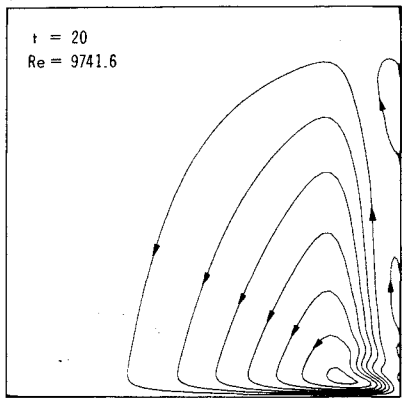

Fig. 8 Instantaneous streamlines at $t=20$; $\psi_{min}=-0.00003$, $\psi_{max}=0.00294$.

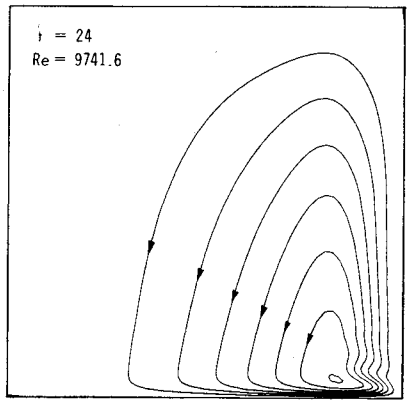

Fig. 9 Instantaneous streamlines at $t=24$; $\psi_{min}=0$, $\psi_{max}=0.00284$.

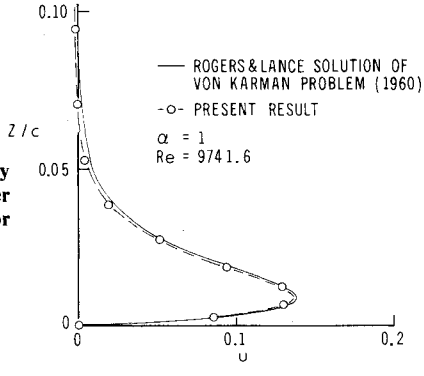

Fig. 10 Radial velocity profile in Ekman layer at $r=0.76$, $t=8.3$ for $\alpha=1$, $Re=9741.6$.

pronounced. Fluid particles near the endwalls are accelerated radially outward in a spiral motion as the Ekman layer develops. These particles overshoot their "equilibrium radial position" before they turn upward from the edge of the Ekman layer near the corner. The reversed flow regions that develop along the sidewall are apparently linked to the inertial oscillations developed as swirling fluid particles travel upward along the sidewall and begin to migrate radially inward.

The calculations predict that as Re increases, both the amplitude of the inertial oscillations and the complexity of the initial flow in the corner region increases. Typical results for $\alpha=1$ and $Re=50{,}000$ show that three very small reversed flow regions develop in the corner region by $t=15$. A transformed 41×81 grid could not sufficiently resolve the fine scales of this motion in the corner. Similar calculations for $\alpha=1$, $Re=100{,}000$ developed a numerical instability at $t=4.6$ due to the extreme severity of the local oscillations in the corner. This result may indicate the development of a physical instability at this high Reynolds number.

Grid convergence studies have been carried out for the case depicted in Figs. 6-9 to determine the sensitivity of the results to grid size. Grids of 11×11, 21×21, and 41×41 were used with $d=e=0.10$ and $\Delta t=0.20$, 0.10, and 0.05, respectively. The results show that the predicted azimuthal velocity profiles are relatively insensitive to grid size. The 41×41 grid results are very similar to those shown in Fig. 6 for the 21×21 grid; typically v differs by less than 0.010 between the two cases, with a maximum difference of 0.027 occurring at early time. The comparisons do show, however, that the number of reversed flow regions formed and their times of appearance and disappearance are sensitive to grid size over this range of sizes. The 11×11 and 21×21 grids are so coarse that only the largest reversed flow region in Fig. 8 is resolved; the smaller ones in Fig. 8 and the single one in Fig. 7 are not resolved at all. All three calculations, however, predict the absence of reversed flow for $t\geq24$. It is clear from these limited results that much finer grids near the sidewall are needed to carry out quantitative studies of the transient reversed flow regions.

Ekman Boundary Layer

The Ekman layer development at early time and its role in the subsequent spin-up process has been examined in some detail using the present procedure. Figure 10 shows a typical computed radial velocity profile in the Ekman layer at $r=0.76$ and $t=8.2$ for $\alpha=1$, $Re=9741.6$. This profile was obtained with a 21×21 grid and $d=0.10$, $e=0.02$. This grid was stretched in z to cluster almost half of the grid points into the Ekman layer. The predicted radial velocity profile is very similar to the one obtained by Rogers and Lance[17] for the steady laminar boundary layer formed on an infinite rotating disk with a nonrotating outer flow (the von Kármán problem). The small differences in Fig. 10 are due to the fact that u does not asymptotically approach zero at the edge of the Ekman layer during spin-up in a finite cylinder. The Rogers and Lance calculation, on the other hand, imposes this asymptotic behavior as a boundary condition.

Results similar to those shown in Fig. 10 have been used to quantify the Ekman layer radial mass flow rate and assess "compatibility conditions" employed in the Wedemeyer model to couple the Ekman layer and interior, or core, flows. These results show that the Ekman layer is formed within approximately the first cylinder rotation, $t=2\pi$; thereafter, the Ekman layer radial mass flow rate at a given r monotonically decreases as t increases. This monotonic behavior of the mass flow rate is an important observation from the present work, since it indicates that non-monotonic compatibility conditions, used by several authors[9,18-20] in conjunction with Wedemeyer's model, are unrealistic approximations to the actual flow. The complete set of numerical results from these studies has been used to develop a new monotonic compatibility condition.[10]

Conclusions

A predictor-corrector multiple-iteration method has been combined with the Gauss-Seidel iteration technique to produce an effective numerical procedure for solving the unsteady Navier-Stokes equations. Test calculations for spin-up in a cylinder were shown to be in good agreement with previous calculations and experimental measurements. Computations carried out for $0.5\leq\alpha\leq4.4$ and $205\leq Re\leq50{,}000$ showed that coordinate transformations could be used to resolve simultaneously details of both the interior and boundary-layer flows using a moderate number of grid points. These calculations demonstrated the presence of inertial oscillations and temporary reversed flow regions along the sidewall during spin-up from rest and quantified some aspects of the flow in the endwall Ekman layers.

Acknowledgment

The advice, encouragement, and assistance of N. Gerber, G. P. Neitzel Jr., and R. Sedney are gratefully acknowledged.

References

[1] Wedemeyer, E. H., "The Unsteady Flow Within a Spinning Cylinder," *Journal of Fluid Mechanics*, Vol. 20, Pt. 3, 1964, pp. 383-399; also, BRL Rept. 1252, Aberdeen Proving Ground, Md., AD 431846, Oct. 1963.

[2] Kitchens, C. W., Jr., Gerber, N., and Sedney, R., "Spin Decay of Liquid-Filled Projectiles," *Journal of Spacecraft and Rockets*, Vol. 15, Nov.-Dec. 1978, pp. 348-354.

[3] Stewartson, K., "On the Stability of a Spinning Top Containing Liquid," *Journal of Fluid Mechanics*, Vol. 5, Pt. 4, Sept. 1959, pp. 577-592.

[4] Rubin, S. G. and Lin, T. C., "A Numerical Method for Three-Dimensional Viscous Flow: Application to the Hypersonic Leading Edge," *Journal of Computational Physics*, Vol. 9, 1972, pp. 339-364.

[5] Salvadori, M. G. and Baron, M. L., *Numerical Methods in Engineering*, Prentice-Hall, Inc., Englewood Cliffs, N.J., 1961.

[6] Warn-Varnas, A., Fowlis, W. W., Piacsek, S., and Lee, S. M., "Numerical Solutions and Laser Doppler Measurements of Spin-Up," *Journal of Fluid Mechanics*, Vol. 85, Pt. 4, 1978, pp. 609-639.

[7] Briley, W. R., "Time Dependent Rotating Flow in a Cylindrical Container," Ph.D. Dissertation, University of Texas at Austin, 1968, University Microfilms, Inc., 69-6121.

[8] Briley, W. R. and Walls, H. A., "A Numerical Study of Time-Dependent Rotating Flow in a Cylinder Container at Low and Moderate Reynolds Numbers," *Proceedings of 2nd International Conference on Numerical Methods in Fluid Dynamics, Lecture Notes in Physics*, Vol. 8, Springer-Verlag, New York, 1970, pp. 377-384.

[9] Watkins, W. B. and Hussey, R. G., "Spin-Up From Rest in a Cylinder," *The Physics of Fluids*, Vol. 20, No. 10, Pt. 1, 1977, pp. 1596-1604.

[10] Kitchens, C. W., Jr., "Navier-Stokes Solutions for Spin-Up from Rest in a Cylindrical Container," ARBRL-TR-02193, Ballistic Research Laboratory, Aberdeen Proving Ground, Md., Sept. 1979.

[11] Neitzel, G. P., Jr., "Centrifugal Instability of Decelerating Swirl Flow within Finite and Infinite Circular Cylinders," Ph.D. Dissertation, Johns Hopkins Univ., Baltimore, Md., 1979.

[12] Roberts, G. O., "Computational Meshes for Boundary-Layer Problems," *Proceedings of 2nd International Conference on Numerical Methods in Fluid Dynamics, Lecture Notes in Physics*, Vol. 8, Springer-Verlag, New York, 1970, pp. 171-177.

[13] Peaceman, D. W. and Rachford, H. H., Jr., "The Numerical Solution of Parabolic and Elliptic Differential Equations," *Journal of S.I.A.M.*, Vol. 3, No. 1, 1955, pp. 28-41.

[14] Young, D., "Iterative Methods for Solving Partial Difference Equations of Elliptic Type," *Transactions of American Mathematical Society*, Vol. 76, 1954, pp. 92-111.

[15] Kitchens, C. W., Jr., Gerber, N., and Sedney, R., "Study of Streamwise Vorticity Decay Downstream of a Three-Dimensional Protuberance," *Bulletin of American Physical Society*, Vol. 20, No. 11, p. 1430.

[16] Williams, G. P., "Numerical Integration of the Three-Dimensional Navier-Stokes Equations for Incompressible Flow," *Journal of Fluid Mechanics*, Vol. 37, 1969, pp. 727-750.

[17] Rogers, M. H. and Lance, G. N., "The Rotationally Symmetric Flow of a Viscous Fluid in the Presence of an Infinite Rotating Disk," *Journal of Fluid Mechanics*, Vol. 7, Pt. 4, April 1960, pp. 617-631.

[18] Weidman, P. D., "On the Spin-Up and Spin-Down of a Rotating Fluid, Pt. 2. Measurements and Stability," *Journal of Fluid Mechanics*, Vol. 77, Pt. 4, 1976, pp. 709-735.

[19] Weidman, P. D., "On the Spin-Up and Spin-Down of a Rotating Fluid, Pt. 1, Extending the Wedemeyer Model," *Journal of Fluid Mechanics*, Vol. 77, Pt. 4, 1976, pp. 685-708.

[20] Goller, H. and Ranov, H., "Unsteady Rotating Flow in a Cylinder with a Free Surface," *Journal of Basic Engineering, Transactions of ASME*, Vol. 90, Series D, Dec. 1968, pp. 445-454.